ISSN 1027-5495. Functional Materials, 28, No.1 (2021), p. 131-137.
doi:https://doi.org/10.15407/fm28.01.131 © 2021 — STC "Institute for Single Crystals"

Dynamic impact compression of lightweight foam concrete

Cao Hai, Ye Qin, Zhou Changjian

School of Civil Engineering and Architecture, Huangshan University,
245041 Huangshan, China

Received July 30, 2020

The performance of dynamic impact compression of lightweight foam concrete under different strain rates was studied using a separate Hopkinson pressure bar. The results show that with an increase in the average strain rate, the fragmentation of the lightweight foam concrete specimens becomes less and less, showing an obvious correlation of the strain rate. The dynamic stress-strain curve of lightweight foam concrete in a one-dimensional stress state can be divided into three stages: linear elastic stage, yield stage and failure stage. The energy absorption by the specimen decreases with an increase in the incident energy and with an increase in the average strain rate of the specimen. There is a power function relationship between them. Due to its low strength, lightweight foam concrete absorbs little total energy and can be effectively used as a protective material.

Keywords: lightweight foam concrete, dynamic impact compression, strain rate, energy absorption rate.

Динамічне ударне стиснення легкого пінобетону. *Cao Hai, Ye Qin, Zhou Changjian.*

Вивчено динамічні характеристики стиснення легкого пінобетону при різних швидкостях деформації за допомогою окремого бару тиску Хопкінсона. Результати показують, що зі збільшенням середньої швидкості деформації фрагментація зразків легкого пінобетону зменшується, демонструючи кореляцію швидкості деформації. Динамічну криву напруга-деформація легкого пінобетону в одновимірному напруженому стані можна розділити на три етапи: етап лінійної пружності, етап плинності і етап руйнування. Через свою низьку міцність легкий пінобетон поглинає мало загальної енергії і може використовуватися як захисний матеріал.

Изучены динамические характеристики сжатия легкого пенобетона при различных скоростях деформации с помощью отдельного бара давления Хопкинсона. Результаты показывают, что с увеличением средней скорости деформации фрагментация образцов легкого пенобетона уменьшается, демонстрируя корреляцию скорости деформации. Динамическую кривую напряжение-деформация легкого пенобетона в одномерном напряженном состоянии можно разделить на три этапа: этап линейной упругости, этап текучести и этап разрушения. Из-за своей низкой прочности легкий пенобетон поглощает мало общей энергии и может использоваться как защитный материал.

1. Introduction

Foam concrete is a kind of closed cell lightweight foam concrete made of ordinary Portland cement, fly ash, silica fume, etc. Foam concrete refers to a kind of porous media material which is first prepared into foam by mechanical method by aqueous solution of foam agent, then added into the slurry composed of siliceous materials (such as sand, fly ash), calcium materials (such as lime, cement), water and other additives, and then mixed, stirred, poured into shape and cured [1-4]. Foam concrete is a kind of

Table 1. Physical performance indicators of lightweight foam concrete

Density, $g \cdot cm^{-3}$	Elasticity modulus, MPa	Compressive strength, MPa	Compression wave velocity, $m \cdot s^{-1}$	Porosity, %	Strain rate, s^{-1}
250	735.2	0.5	1924	92.1	10000

porous medium material with an internal uniform distribution of a large number of tiny pores. Chen Bing [5] studied the effects of microsilica powder and polypropylene fiber on the compressive strength, splitting tensile strength and shrinkage rate of foamed concrete with a density of 800 kg/m^3 to 1500 kg/m^3. Fang Yonghao [6] studied the relationship between compressive strength and pore structure of cement-fly ash foam concrete and obtained a corresponding mathematical expression. Devid Falliano et al. [7] showed that the water/cement ratio had a great influence on the compressive strength of foamed concrete. Different foaming agents lead to different void arrangement in the microstructure of the product. Compared to curing in glass paper, curing in air provides the lowest compressive strength. Ramamurthy et al. [8, 9] showed that the volume of stomata, their diameter and spacing between stomata affect the density and intensity of the stomata, regardless of their shape. The influence of sulfate on the loss of strength, expansion and quality of foam concrete is also analyzed.

More and more attention is paid to the study of the impact characteristics of foam concrete as a kind of lightweight shockproof energy-absorbing material [10]. Yuan Pu et al. [11] carried out the dynamic compression test of cellular porous concrete at an approximately constant strain rate. Li Ran [12] studied the dynamic loading of 6 types of cellular concrete with different densities under high strain rate by using the aluminum separated Hopkinson compression bar system with diameter of 75 mm; it was established that the maximum failure stress and elastic modulus of cellular concrete increase with a decrease in the porosity under high strain rate.

In order to fully understand the various properties of foam concrete and expand its application scope, it is necessary to thoroughly and deeply study the various properties of foam concrete. Currently, the density of foam concrete most widely studied and applied in the country and abroad is usually 300 ~ 1200 kg/m^3, and the research mainly focuses on the thermal and static mechanical properties. Due to its large deformation, high inhomogeneity and viscoplasticity, little research has been done on its dynamic mechanical properties [11].

Ultra-light foamed concrete with a density of less than 300 kg/m^3 demonstrates technical advantages in external wall insulation systems, roof insulation engineering, lightweight cushion, floor heating engineering and for energy-saving composite hollow blocks. For this reason, the dynamic characteristics of about 250 kg/m^3 foam concrete were studied by a separated Hopkinson compression bar (SHPB) system. The mechanism of shock resistance and energy absorption is discussed, which provides a theoretical basis for the design of a new composite protection structure.

2. Experimental

Foam concrete is evenly mixed with ordinary Portland cement, fly ash, silica smoke and poured into a foam mixture consisting of a homogeneous suspension; after foaming, holding, cutting and other technologies, cellular lightweight foam concrete is poured into the mold. Ultra-lightweight foam concrete with density about 250 kg/m^3 has low density, low mechanical impedance, uniform bubble, etc. The porosity of the foam concrete is very high, there are a lot of pores in the sample; pore walls are very thin and the pore diameter is much larger than the thickness of the pore wall. Its physical performance indicators are shown in Table 1.

The system of dynamics tests on a SHPB device with a diameter of 37 mm was used. The impact bar, incident bar and transmission bar are all made of steel. The elastic modulus is 210 GPa, the density is 7.8 g/cm^3, and the velocity of longitudinal wave is 5190 m/s. The length of impact bar is 600 mm; the length of the incident bar is 2400 mm; the transmission bar length is 2000 mm. The test device is shown in Fig. 1.

The basic principle of SHPB testing is that the high pressure released gas instantaneously pushes the impactor against the incident bar, thus generating an elastic compression wave propagating on both sides

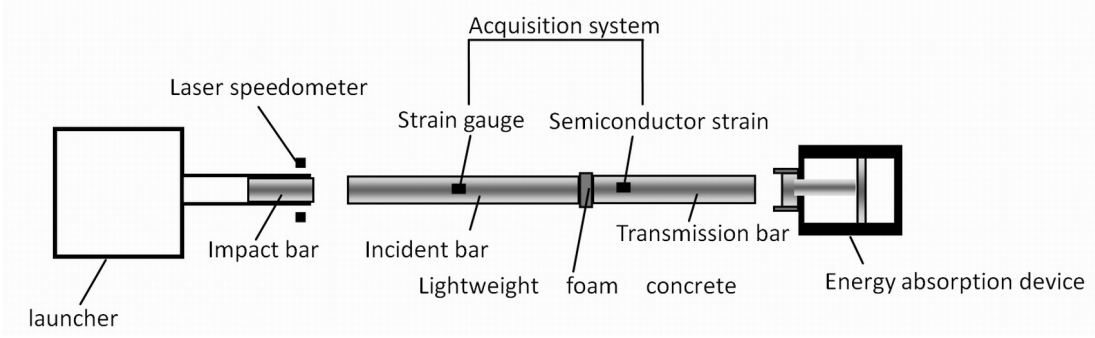

Fig. 1. Split Hopkinson pressure bar apparatus.

of the impactor [13]. When the reflected shock tensile wave returns, the impact bar is separated from the incident bar, and the rectangular stress pulse is propagated forward in the press bar from one side of the incident bar to the other, and the stress wave generated by this incident bar is called the incident wave. When the stress pulse propagates to the specimen, the specimen deforms rapidly under the impact of the stress pulse, and the incident bar reflects a part of the stress wave, that is, the reflected wave. Another part of the stress wave propagating to the transmission bar is called the transmission wave. In the elastic range, the faster the impact velocity, the greater the stress pulse amplitude. In SHPB testing, the impact velocity can be controlled by adjusting the air pressure and the impact stroke of the impact bar, and different stress pulse amplitudes and loading speeds can be realized.

The basic assumption of SHPB testing is as follows: during the test, the bar generates and propagates a one-dimensional elastic stress wave; the strain and stress of the specimen are uniformly distributed along the length axis [14]. Under the action of the stress wave generated by the compression bar, the specimen will rapidly expand in the radial direction and contract in the axial direction, resulting in a test error. The measurement error increases with an increase in the stress pulse, which is called the inertia effect. Pankow M. et al. [15] obtained cylindrical concrete specimens with a length-diameter ratio of 0.5, which greatly reduced the test error generated by the inertial effect and could ignore the adverse impact of the inertial effect. In this test, the length-diameter ratio of specimen is 0.5, that is, the bottom diameter of concrete cylinder specimen was 37 mm and the height was 18 mm, meeting the requirement of the length-diameter ratio of specimen, as shown in Fig. 2.

Fig. 2. Specimen for testing.

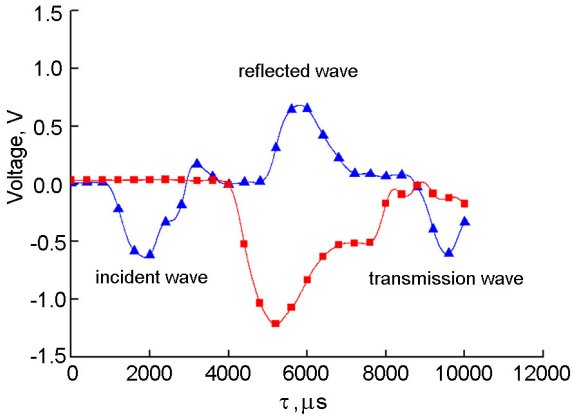

Fig. 3. Typical waveforms.

When the friction coefficient between the end face of the press bar and the part to be tested is less than 0.065, the error caused by the friction effect on the test can be less than 5 %. Since the surface of the specimen must be smooth, vaseline is evenly applied to the two surfaces of the specimen, so that the end face of the device press bar is in close contact with the specimen, thereby reducing the negative friction effect. In order to collect a strong strain signal, the strain gauges are usually glued in the middle of the SHPB incident bar and at the end of the SHPB transmission bar, close to the tested concrete specimen. Therefore, the strain gauge on the incident bar was glued in the middle of the rod, that is, 1200 mm away from the specimen to be

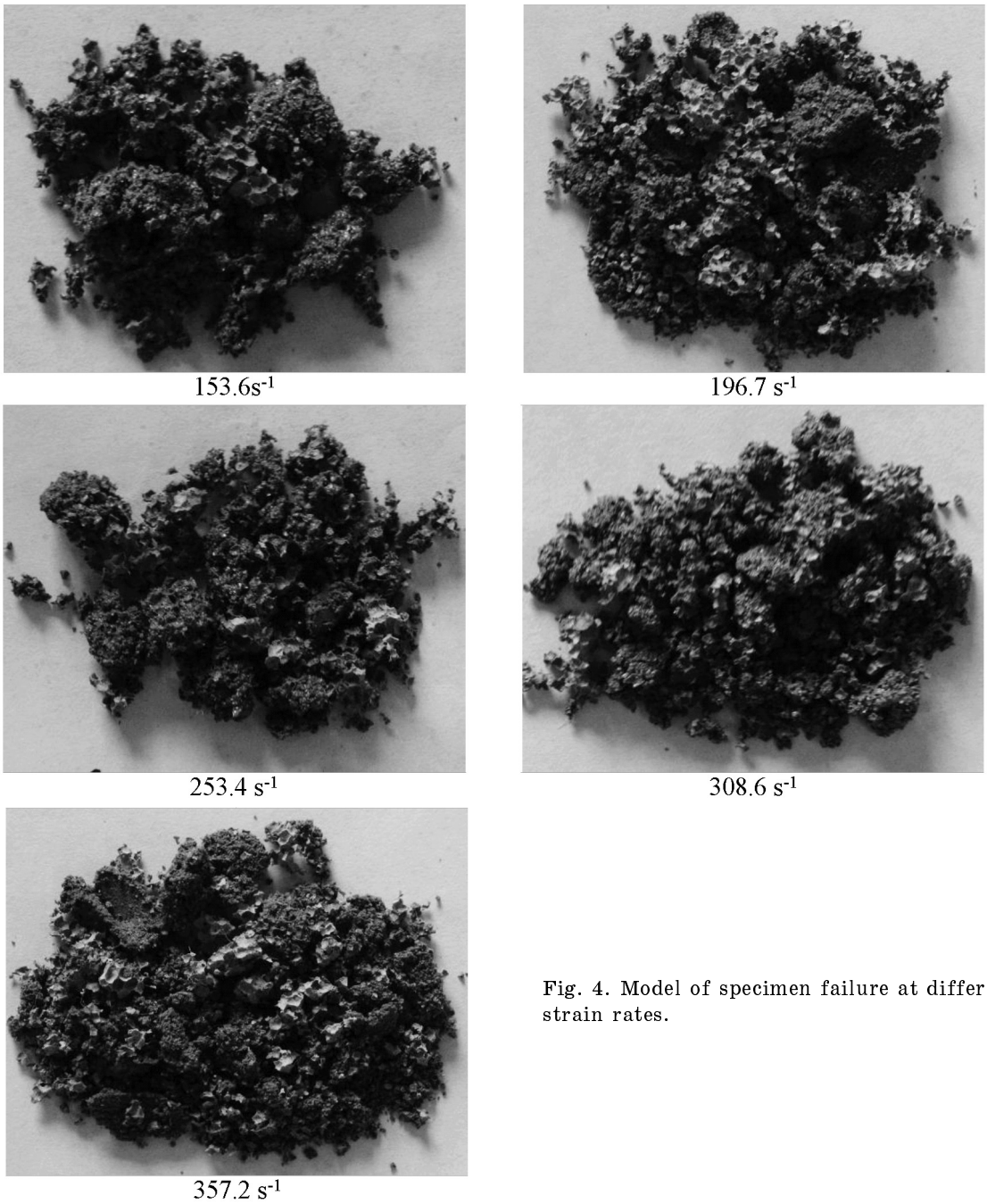

Fig. 4. Model of specimen failure at different strain rates.

tested. The strain gauge on the transmission bar was glued at a distance of 200 mm from the specimen to be tested. The original waveform collected in the test is shown in Fig. 3. It can be seen that the measured waveform is relatively smooth, which allows a semi-normal wave loading to be realized.

3. Results and discussion

Based on the two basic assumptions in the SHPB test, the originally collected waveforms were processed using the simplified three-wave method [16, 17], and the following expressions for stress $\sigma(t)$, strain $\varepsilon(t)$ and strain rate $\dot{\varepsilon}(t)$ were obtained:

$$\sigma(t) = \frac{E_0 A_0}{A_s}\varepsilon_T(t), \tag{1}$$

$$\varepsilon(t) = \frac{C_0}{l_s}\int_0^\tau [\varepsilon_I(t) - \varepsilon_R(t) - \varepsilon_T(t)]dt, \tag{2}$$

$$\dot{\varepsilon}(t) = \frac{C_0}{l_s}[\varepsilon_I(t) - \varepsilon_R(t) - \varepsilon_T(t)]. \tag{3}$$

Here, $\varepsilon_I(t)$, $\varepsilon_R(t)$ and $\varepsilon_T(t)$ are respectively the incident, reflected and transmission stress waves at time t; E_0, A_0, C_0 and A_s are respectively the elastic modulus, cross section area, longitudinal wave velocity in the bar and cross section area of the specimen; $C_0 = \sqrt{E_0/\rho_0}$, ρ_0 is the density of the bar material; l_s is the height of the specimen; τ is the duration of stress wave.

3.1. Failure morphology

As a result of testing by the SHPB method, the fracture morphology of lightweight foam concrete at various strain rates was obtained, as shown in Fig. 4. The analysis of the dynamics of fracture morphology of lightweight foam concrete specimens shows that in the SHPB testing under uniaxial compression, with an increase in the average strain rate, the fragmentation of lightweight foam concrete specimens becomes less and less. During the test, it was found that the samples of the input bar end and the output bar end in contact with both ends of the SHPB bar and the lightweight foam concrete specimen were crushed into powder, and the materials near the middle of the specimen were broken into fragments and shot out due to the transverse deformation of the materials.

3.2. Stress-strain curve

Lightweight foam concrete is a typical porous engineering material, which is easy to prepare, low cost and has certain building strength. In the test, a separated Hopkinson bar device with a diameter of 37 mm was adopted to control the bar velocity by setting different impact pressure, and the stress-strain curves of lightweight foam concrete specimens with different strain rates under one-dimensional stress were measured, as shown in Fig. 5.

It can be seen from the measured stress-strain curve that the elastic limit of lightweight foam concrete is very low, less than 1 MPa, generally only a few tenths. At first, there is a linear stress-strain relationship; when the dynamic load increases, the maximum is observed which can be considered as the elastic limit of material; then the material strength begins to decline, but the rate of strength degradation drops slowly showing an obvious yield platform (at the average strain rate of 196.7 s^{-1}) before it begins to fall. The dynamic stress-strain curve of lightweight foam concrete in a one-dimensional stress state is mainly divided into three stages: the stage of linear

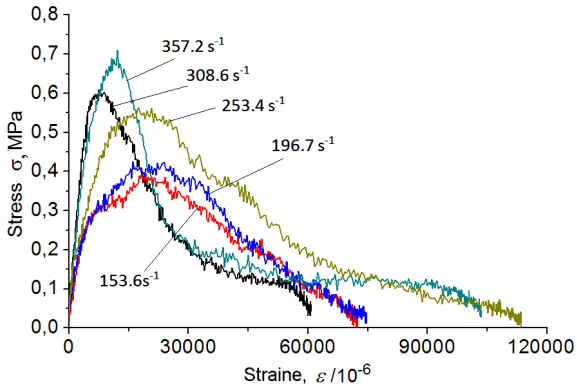

Fig. 5. Experimental stress-strain curves of lightweight foam concrete specimens.

elasticity, the stage of yield and the stage of destruction [18, 19].

The first stage is the stage of linear elasticity. At the beginning, the pore wall skeleton of the lightweight foam concrete specimen had a certain bearing capacity. At this stage, the load is taken up by the pore wall skeleton, and the relationship between stress and strain is basically linear, in line with Hooke's law in mechanics. Part of the energy of the incident stress wave was converted into the elastic deformation energy of the specimen.

The second stage is the yield stage. When the external load continues to increase and exceeds the bearing capacity of the pore wall skeleton of the foamed concrete specimen, the pore wall begins to fracture brittle, but the specimen still has a certain bearing capacity. At this point, part of the incident stress wave energy is converted into the plastic deformation energy of the specimen.

The third stage is the failure stage. The pores in the lightweight foam concrete are gradually compacted, and when the pore wall is completely destroyed or the pores are completely compacted, the specimen no longer bears the load.

3.3. Energy absorption

Assuming that the energy loss at the contact between the specimen and the input bar and the output bar section is ignored, the energy absorbed by the specimen can be calculated as follows:

$$W_S = W_I - (W_R + W_T\}, \qquad (4)$$

where W_S, W_I, W_R, and W_T are respectively the absorption energy, incident energy, reflected energy and transmission energy.

For lightweight foam concrete, a kind of low mechanical impedance material, the dif-

Table 2. Energy analysis of lightweight foam concrete

No.	Diameter, mm	Height, mm	Strain rate, s^{-1}	Incident energy, J	Reflected energy, J	Specimen absorbed energy, J	Energy absorption rate
1	37.2	18.7	153.6	13.125	12.567	0.558	0.043
2	36.8	18.2	196.7	19.278	18.652	0.626	0.032
3	36.7	18.4	253.4	35.249	34.546	0.703	0.020
4	36.9	18.9	308.6	58.751	58.025	0.726	0.012
5	36.4	18.1	357.2	81.246	80.358	0.888	0.011

ference between the incident waveform and the reflected waveform measured in the test is not large. Here, the uniformity assumption $\varepsilon_T(t) = \varepsilon_I(t) + \varepsilon_R(t)$ is introduced; then the above formula becomes:

$$W_S = W_I - (W_R + W_T) =$$

$$= \frac{AC_0}{E}\left(\int\sigma_I^2 dt - \int\sigma_R^2 dt - \int\sigma_T^2 dt\right) =$$

$$= \frac{AC_0}{E}\left[\int(\sigma_T - \sigma_R)^2 dt - \int\sigma_R^2 dt - \int\sigma_T^2 dt\right] =$$

$$= \frac{AC_0}{E}\left[\int(\sigma_T^2 + \sigma_R^2 - 2\sigma_T\sigma_R)dt - \int\sigma_R^2 dt - \int\sigma_T^2 dt\right] =$$

$$= -\frac{AC_0}{E}\int 2\sigma_T\sigma_R dt.$$

That is, the absorption energy is:

$$W_s = -\frac{AC_0}{E}\int 2\sigma_T\sigma_R dt, \qquad (5)$$

where σ_I, σ_R and σ_T are respectively the time behavior of the incident stress wave, the time behavior of the reflected stress wave and the time behavior of transmission stress wave.

In order to study the energy absorption capacity of lightweight foaming concrete specimens at different strain rates, a dimensionless physical quantity, energy absorption rate (EAR), was introduced for the study, and was defined as the ratio of energy absorbed by the specimens to the energy of the incident stress wave. The calculation formula was as follows:

$$EAR = W_S / W_I. \qquad (6)$$

From the energy analysis (Table 2) it can be seen that the specimens absorb very little energy under dynamic loading; the maximum energy absorption rate was only 4.3 %, most of the incident energy was reflected back because of the mismatch between wave impedance of the specimen and the elastic compression bar; the ratio of the wave impedance between the sample and the compression bar measured in the experiment is 0.031, and the reflected energy measured was at least 95.7 % of the incident energy, usually in more than 98 %. Therefore, for lightweight foam concrete, which is a low impedance material, the energy dissipation mechanism is to reflect most of the energy away from it, rather than absorbing the energy of the material itself. At the same time, with an increase in the impact bar velocity, the energy of the incident stress wave increases and the absorption energy of the specimen increases, but the energy absorption rate of the specimen decreases. It can also be found that the energy passing through the lightweight foam concrete specimen is so small that it can be almost ignored. Therefore, lightweight foam concrete can be used as an effective protective material, which is also a good anti-knock and shockproof material.

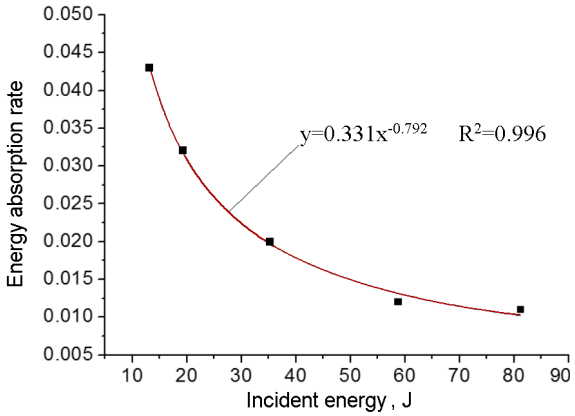

Fig. 6. Relationship between incident energy and energy absorption rate.

The variation of the energy absorption rate depending on the incident energy for a lightweight foam concrete specimen is shown in Fig. 6. The curve in the figure is formed by fitting a power function to the measured data points. By analyzing the data in Fig. 6, it can be found that the energy

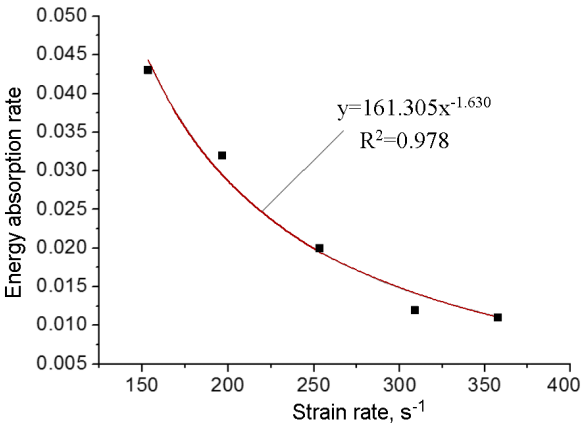

Fig. 7. Relationship between strain rate and energy absorption rate.

absorption rate of lightweight foam concrete decreases with an increase in the incident energy.

Fig. 7 shows the change of the energy absorption rate of the specimen vs the average strain rate under different strain rates. The curve in the figure is formed by fitting a power function to the measured data points. Absorption energy of the specimen decreases with an increase in the average strain rate; this is due to the fact that with an increase in the deformation rate, an increase in the strength of lightweight concrete is not obvious. The added absorption energy of the specimen is much lower than the incident energy; therefore a negative correlation is shown between the rate of energy absorption and the average strain rate of the specimen.

4. Conclusions

By using the semiconductor strain gauge with high sensitivity coefficient and vaseline as the incident pulse shaper, the problem of difficulties in collecting the transmitted signal of the porous lightweight foam concrete with low impedance was solved, and the stress uniformity of the specimen was achieved during the loading process.

With an increase in the average strain rate, the fragmentation of the lightweight foam concrete specimens becomes less and less, showing an obvious strain rate effect.

Under the impact compression load, the dynamic stress-strain curve of lightweight foam concrete successively passes through the linear elastic stage, the yield stage and the failure stage.

Due to their low strength, lightweight foam concrete specimens absorb little total energy. The energy dissipation mechanism is to reflect most of the energy from the specimens, rather than absorbing the energy by the materials themselves, which can effectively protect the objects.

The energy absorption rate decreases with an increase in the incident energy and average strain rate. And there is a power function relation between them.

Acknowledgements. This paper is funded by Excellent Young Talent Support Program for Universities in Anhui Province (gxyq2020050)?Talent program of Huangshan University (2018xkjq012) and the innovation training projects for college students (S202010375008?S201910375063).

References

1. Tian Guoxin, Huang Jun, *Concrete*, 3 (2017).
2. Y.H.M.Amran, N.Farzadnia, A.A.A.Ali, *Constr.Build. Mater., Part 1, 101 (2015)*.
3. K.Ramamurthy, E.K.K.Nambiar, G.I.S.Ranjani, *Cement Concrete Comp*, **6**, 31 (2009).
4. E.P.Kearsley, P.J.Wainwright, *Cement Concrete Res.*, **2**, 32 (2002).
5. Chen Bing, Liu Jie. *J.Build. Mater.* **3**, 13 (2010).
6. Fang Yonghao, Wang Rui,Pang Erbo et al., *J.Chinese Ceram. Soc.*, **4**, 38 (2010).
7. Devid Falliano, Dario de domenico, Giuseppe Ricciardi et al., *Constr.Build. Mater., 165 (2018)*.
8. E.K.Kunhanandan Nambiar, K.Ramamurthy, *Cement. Concr. Res*, **2**, 37 (2007).
9. G.Indu Siva Ranjani, K.Ramamurthy, *Cement Concr. Comp.*, **7**, 34 (2012).
10. Lili Wang, *Expl. Shock Waves*, **2**, 21 (2001).
11. Pu Yuan, Qinyong Ma, Haidong Zhang, *J.Vibr. Shock*, **17**, 33 (2014).
12. Haiyan Liu, Ran Li. *J. Chengdu Univ. (Natural Sci. Edit,)*, **2**, 29 (2010).
13. Tongxi Yu, Xingming Qiu, Impact Dynamics, Tsinghua University Press, Beijing (2011).
14. Lili Wang, Foundation of Stress Waves (2nd ed.), National Defense Industry Press, Beijing (2010).
15. M.Pankow, C.Attard, A.M.Waas, *J. Strain Anal. Engin.Design*, **8**, 44 (2009).
16. Li Song, Shisheng Hu, *Expls. Shock Waves*, **4**, 25 (2005).
17. Lili Wang, Foundation of Stress Waves, Elsevier, Amsterdam (2007).
18. Kai Zhao, Xiao Jun Wang, Fei Liu et al., *Expls. Shock Waves*, **1**, 31 (2011).
19. L.J.Gibson, M.F.Ashby, Cellular Solids, Structure and Properties, Cambridge University Press, London (1997).